

UVic-PUMA (OSU)

Documentation of the coupled climate model

Andreas Schmittner¹ and Tiago Silva²

College of Oceanic and Atmospheric Sciences, Oregon State University, Corvallis OR, USA.

¹ aschmitt@coas.oregonstate.edu

² now at University of East Anglia, UK.

Introduction

Both the UVic model and the PUMA model have an extensive history and documentation. We refer to the web sites (<http://climate.uvic.ca/> and <http://www.mi.uni-hamburg.de/6.0.html>) for further information. Here, only information pertinent to the coupling and the coupled model performance is described.

Coupling

A total of 15 fields (Figure 1) are exchanged between the models at each coupling timestep Δt_{CPL} . Liquid (P_l) and solid (P_s) precipitation, specific humidity (q_{2m}) and air temperature (T_{2m}) at 2 m, meridional and zonal wind stress components (τ_x, τ_y), wind speed ($|u|$), and the downward components of the surface shortwave (F^{SWd}) and longwave radiation (F^{LWd}) are passed from PUMA to UVic (blue arrows). Surface temperature (T_{sfc}), roughness length (z_0), sensible heat flux (F^{SH}) and evaporation (E), surface albedo (a_{sfc}) and the upward component of the surface longwave radiation are passed from UVic to PUMA (red arrows). First order conservative remapping is used for the fluxes from UVic to PUMA ($E, F^{SH}, F^{SWu}, F^{LWu}$), and second order conservative remapping is used for the fluxes from PUMA to UVic ($P_l, P_s, \tau_x, \tau_y, F^{SWd}, F^{LWd}$) [Jones, 1999]. For those variables that do not need to be conserved bilinear interpolation is used ($T_{2m}, q_{2m}, |u|, T_{sfc}, z_0$).

Calculation of $P_l, P_s, \tau_x, \tau_y, F^{SWd}, F^{LWd}$ is according to the PUMA schemes [Lunkeit *et al.*, 2007] and $E, F^{SH}, F^{SWu}, F^{LWu}$ are calculated using UVic's formulas [Weaver *et al.*, 2001]. It might be desirable in the future to update the calculation of the fluxes in UVic with the PUMA boundary layer scheme, which considers stratification.

At the end of the shortwave routine in PUMA the upcoming shortwave radiation at the surface $F^{\uparrow SW}$ is replaced by the UVic flux. The surface albedo is diagnosed according to $R_s = F^{\uparrow SW} / F^{\downarrow SW}$ and used in the subsequent call to the radiation scheme. The longwave flux emitted from the surface $A_s B(T_s)$ (see equation 3.56 in Plasim Manual) is replaced by the UVic flux. The surface emissivity is diagnosed

according to $A_s = F_{UVic}^{\uparrow LW} / B(T_s)$ and then used to calculate the reflected component of the up going longwave radiation $(1 - A_s)F_{L+1}^{\downarrow LW}$.

The time stepping scheme is shown in Figure 2. Different time steps are used. The atmospheric time step is the shortest. At T21 resolution $\Delta t_A=45$ min, and at T42 resolution $\Delta t_A=20$ min is used. The sea ice and land surface models use a time step of $\Delta t_{IL}=7.5$ h and the ocean model uses a time step of $\Delta t_o=30$ h for the advection of tracers. Fluxes are exchanged between the atmosphere and the sea ice/land surface every two land/ice time steps $\Delta t_{CPL}=2 \times \Delta t_{IL}=15$ h (T21). Fluxes between the ocean and the sea ice and atmosphere are exchanged every $\Delta t_{CPO}=2 \times \Delta t_o=60$ h=2.5 d.

Currently three CPUs are used, one for PUMA, one for OASIS and one for UVic. During each ocean coupling time step Δt_{CPO} the following sequence is used (see Figure 3). (1) Initially the atmosphere and the ocean models run parallel. (2) Fields are passed - either directly from the ocean or via OASIS from the atmosphere - to the surface (land/ice) model. (3) The surface model integrates two time steps, during which the ocean and atmosphere models wait for input. (4) Information is passed to the atmosphere. (5) The atmosphere is stepped forward for $\Delta t_{CPL}/\Delta t_A$ time steps. (6) Fields are passed from the atmosphere to the surface model. (7) The surface model runs two time steps and (8) passes information to atmosphere and ocean.

Comparison with Observations

The figures below show runs of model version 0.2. Initial test runs showed that the default PUMA parameter setting leads to a too cold climate and too little global cloud cover. Therefore some PUMA parameter values have been adjusted from the default setting. In particular the cloud albedo has been increased (TSWR1=0.03, TSWR2=0.033, TSWR3=0.06) and the critical humidity for cloud formation has been set to decrease from 0.86 at the surface to 0.76 at the TOA. These changes lead to global mean SSTs and cloud cover close to observations. The T21 version has been run for more than 1700 years the T42 version for ~300 years. The deep ocean is still experiencing strong drift in the T42 version but the T21 version is close to equilibrium (Figure 4). The surface in T42 is close to a statistically steady state. A considerable imbalance (-3 W/m²) remains at the top of the atmosphere (TOA) even after 1700 years in the T21 version. A similar imbalance is found in the PUMA stand-alone version. In the tropics incoming solar radiation is 10-20 W/m² to small, whereas it is overestimated at mid and high latitudes (Figure 5). The planetary albedo is too large at low latitudes, particularly over the oceans (Figure 7), whereas it is too small at mid latitudes between 40-70°N/S.

The surface albedo is in good agreement with observations over the oceans (Figure 9), which implies that the cloud albedo causes the biases of the planetary albedo over sea ice-free (<60°N/S) oceans. Cloud cover (Figure 11) is too low over the central and eastern equatorial Pacific, the equatorial Atlantic, and the western Indian ocean along the east coast of Africa, explaining the overestimated planetary

albedo there. However, between about 10-30° cloud cover is underestimated and therefore does not explain the too high planetary albedo. This implies that the cloud albedo is too high there.

Cloud cover is underestimated over large areas of the extratropical ocean. Interestingly this bias seems to be larger in the higher resolution model (Figure 12), where as the bias in the planetary albedo is smaller in T42 compared with T21, suggesting the cloud albedo is lower – and in better agreement with the observations – in T42 than in T21.

The largest bias in the zonally averaged air temperature – besides the warm bias in the low latitude stratosphere – is a strong cold bias in the Arctic in both model versions (Figure 13-14).

Surface air temperatures also show the strong cold bias over the Arctic (Figure 15), particularly in winter (Figure 17). North of 70° the air is 30°C too cold!

The cold bias over the ocean is worse in the lower resolution model, possibly due to the overestimated cloud albedo.

Precipitation is reasonable in both models, with the exception of a wet bias over the eastern subtropical ocean basins (Figure 21). T42 has a double ITCZ. Precipitation over the West Pacific Warm Pool is underestimated, suggesting a too weak Walker circulation.

Zonal wind stress over the ocean is much better in T42 than in T21. Particularly over the Southern Ocean wind stress is much too weak in T21 and the maximum of the westerlies is much too far north. This leads to too little Ekman divergence, underestimated upwelling and too small sea ice area. The latter is the reason for the warm bias in the T21 version in the subpolar Antarctic.

In overturning in the Atlantic has been highly variable during the first 120 years of the T21 model run (Figure 31). The ACC is around 130 Sv in both models, but it can be expected to change as the ocean states equilibrate more.

There's a strong cold bias at much of the ocean surface, particularly in the subtropical gyres of the northern hemisphere (Figure 32).

The surface net shortwave radiation is mostly overestimated (Figure 34). This seems to be inconsistent with the overestimated planetary albedo over the low latitude oceans (Figure 7), but might be consistent with the underestimated cloud cover (Figure 11). ???

Biases in the surface net longwave radiation are generally small over the oceans (Figure 36), as are biases in the sensible heat flux (Figure 38).

Evaporative cooling (Figure 40) is generally too large over the oceans and seems to be balancing the overestimated shortwave (Figure 34).

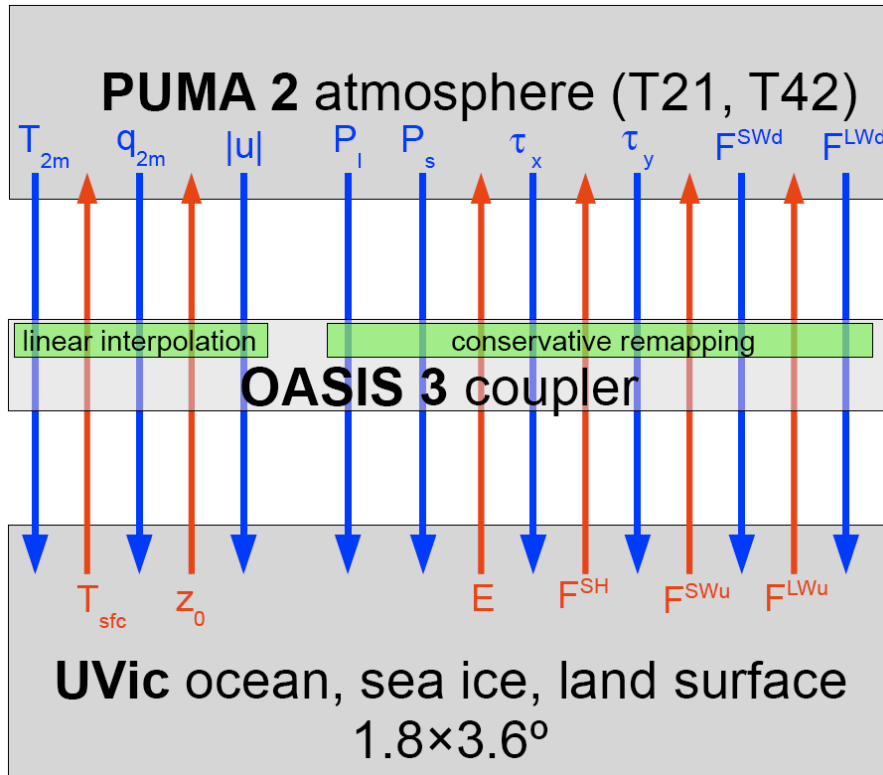


Figure 1: Fields exchanged between the UVic model and PUMA. The OASIS (version 3) coupler is used for conservative remapping of surface fluxes between the different model grids. Other variables that are required in one model from the other model, e.g. in the calculation of surface fluxes or for the convection scheme, are linearly interpolated between the model grids.

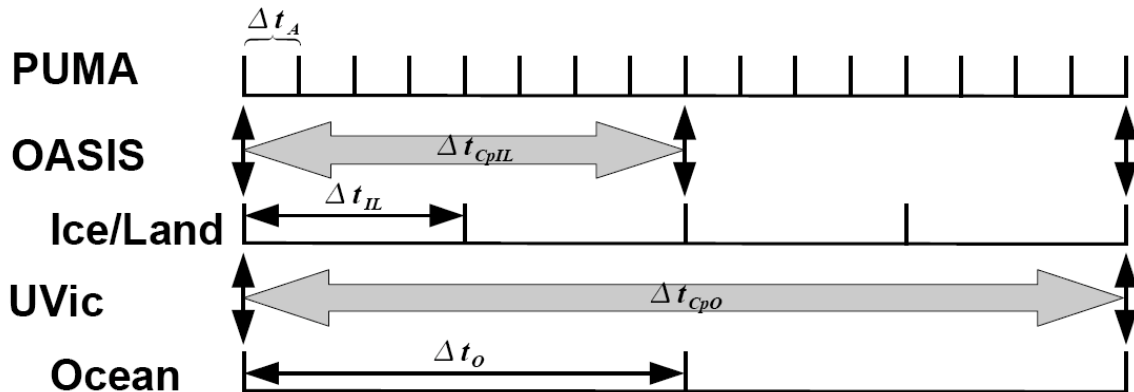


Figure 2: Time stepping of the coupled model.

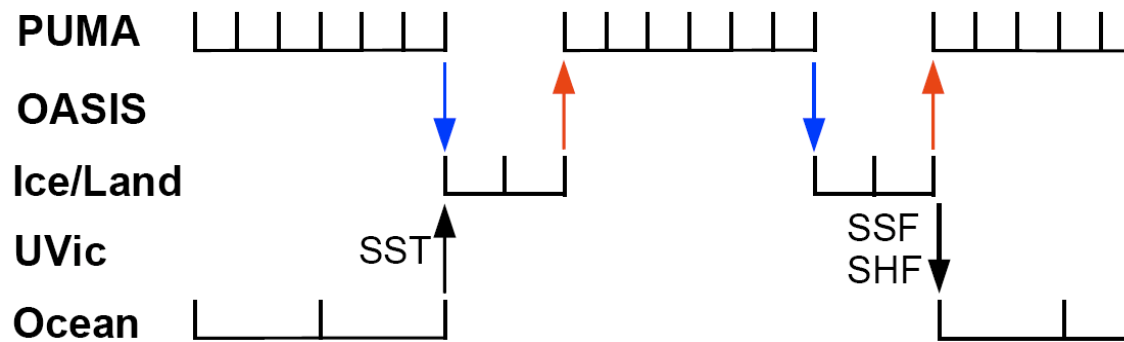


Figure 3: Coupling sequence. Each ocean coupling time step the ocean passes SST to the ice and receives surface salt flux (SSF), surface heat flux (SHF) and momentum fluxes (wind stress). The red and blue arrows correspond to those of Figure 1.

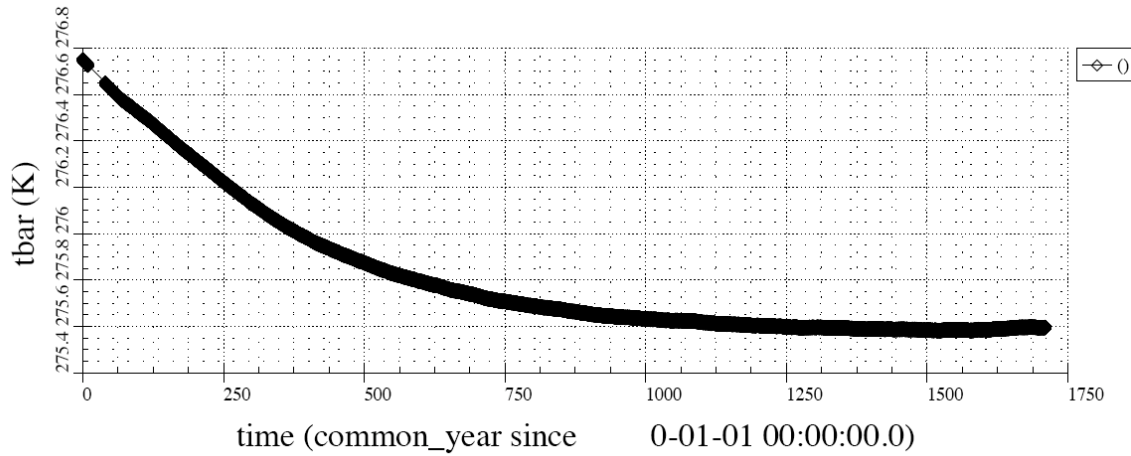


Figure 4: T21 Global average ocean temperature.

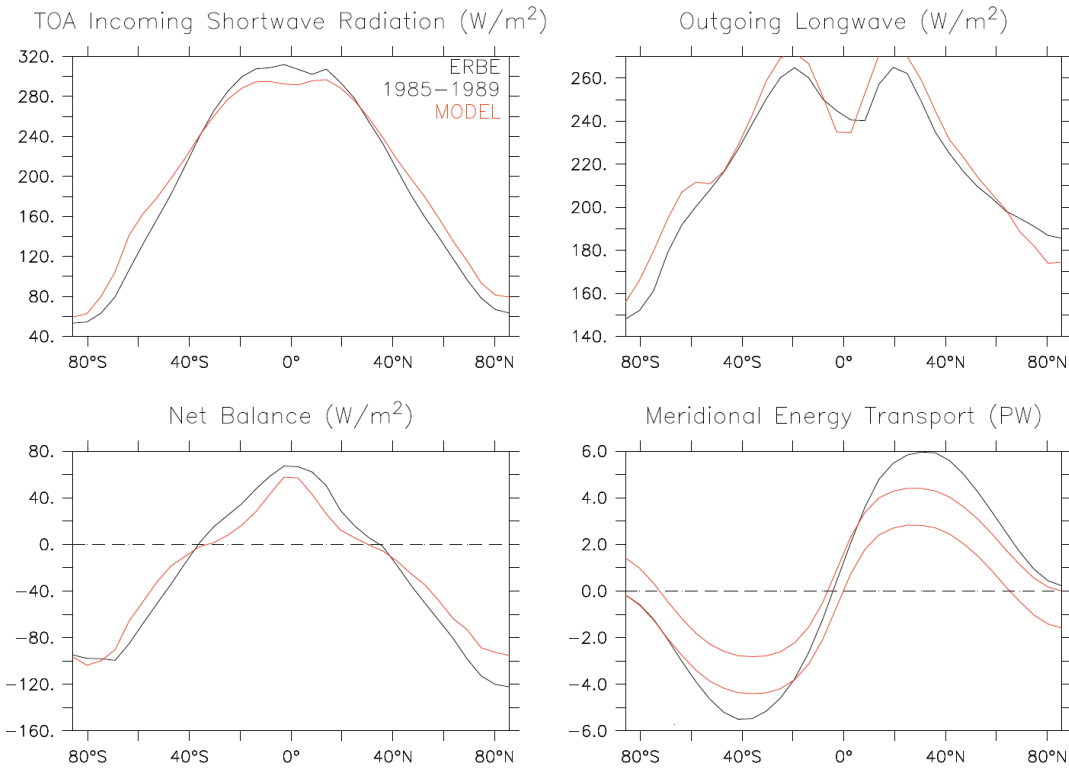


Figure 5: T21 TOA fluxes. The meridional heat flux was calculated by integration of the TOA net flux. Upper line starts from north pole, lower line from south pole. Difference is due to global imbalance (=error).

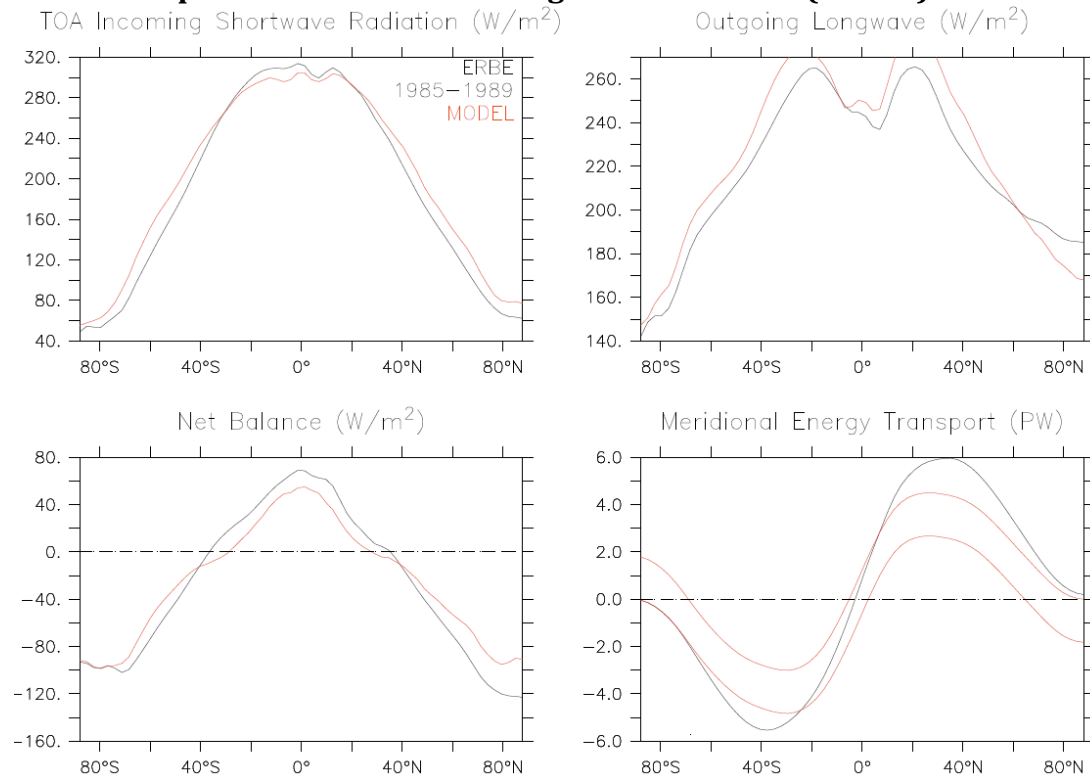


Figure 6: T42 TOA fluxes.

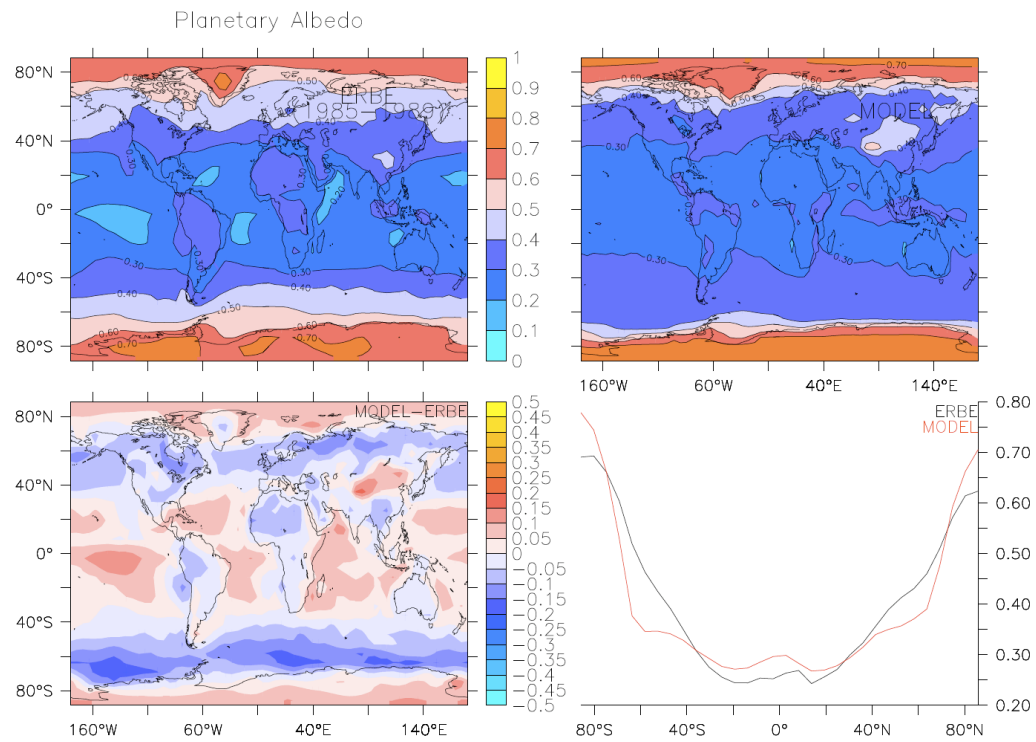


Figure 7: T21 Planetary albedo.

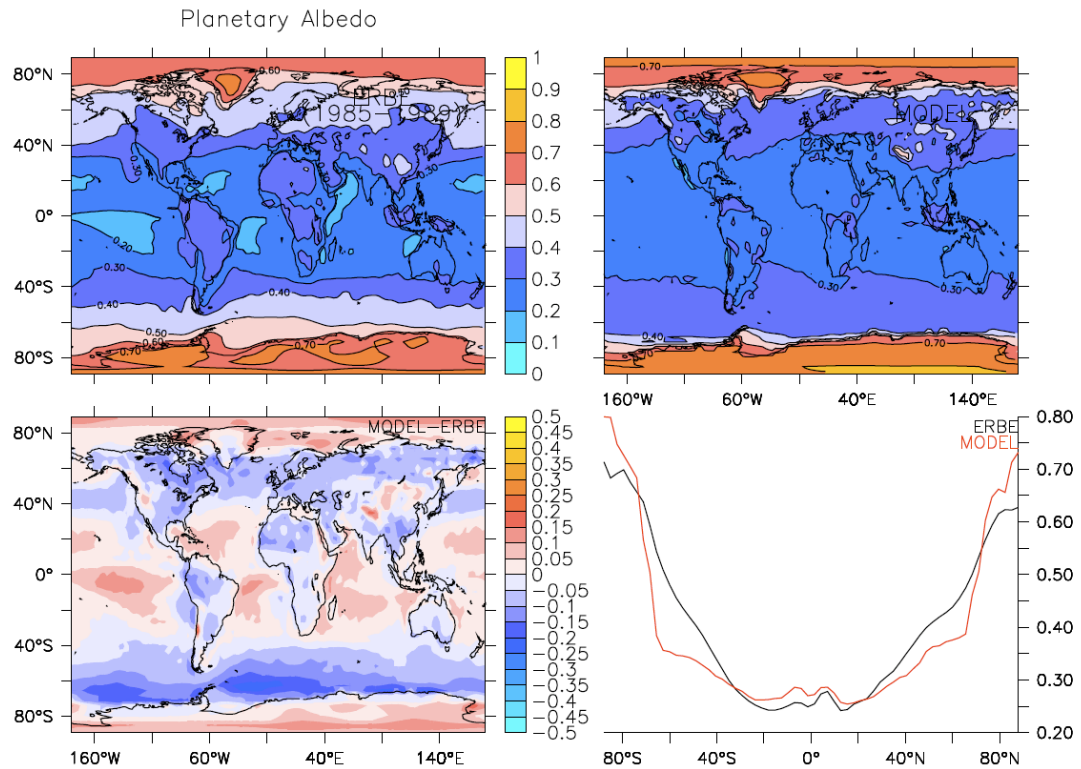


Figure 8: T42

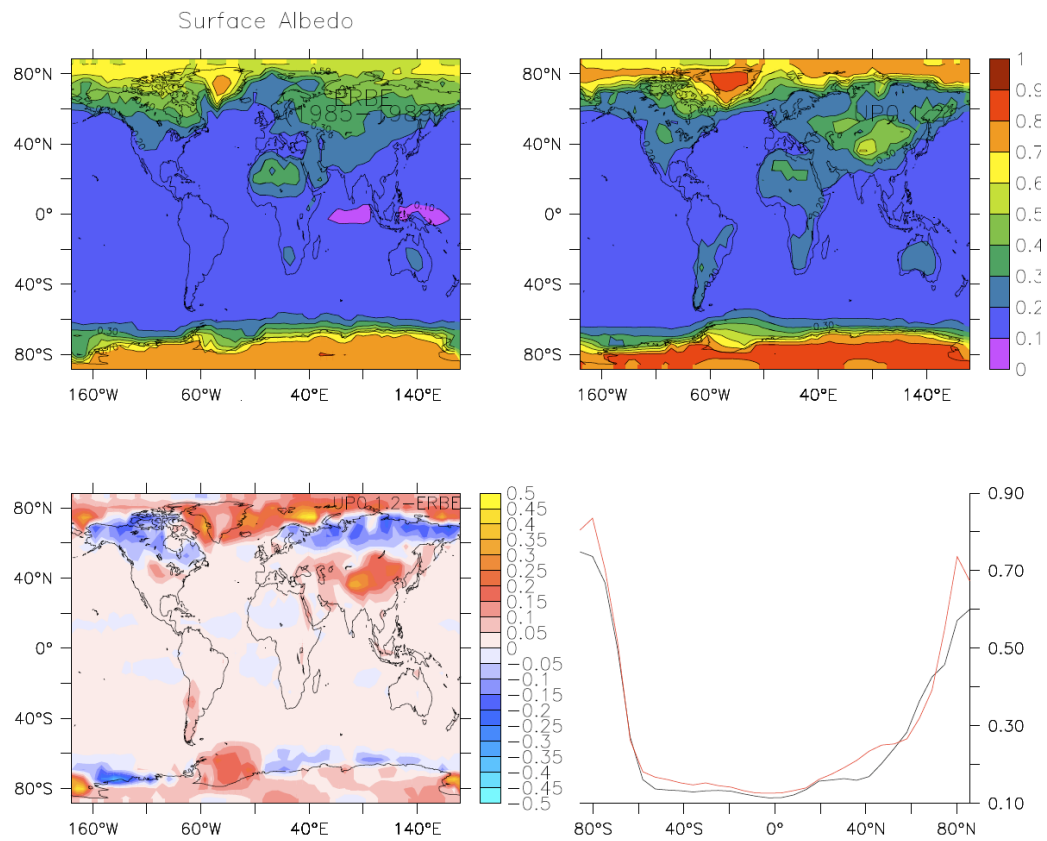


Figure 9: T21 Surface albedo.

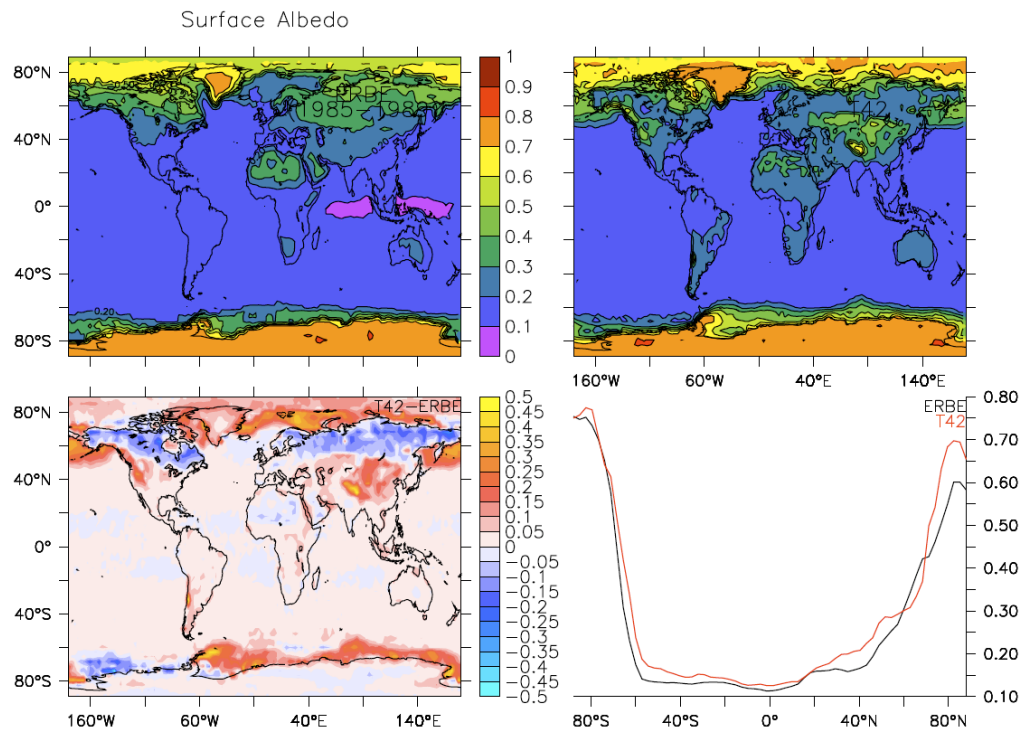


Figure 10: T42

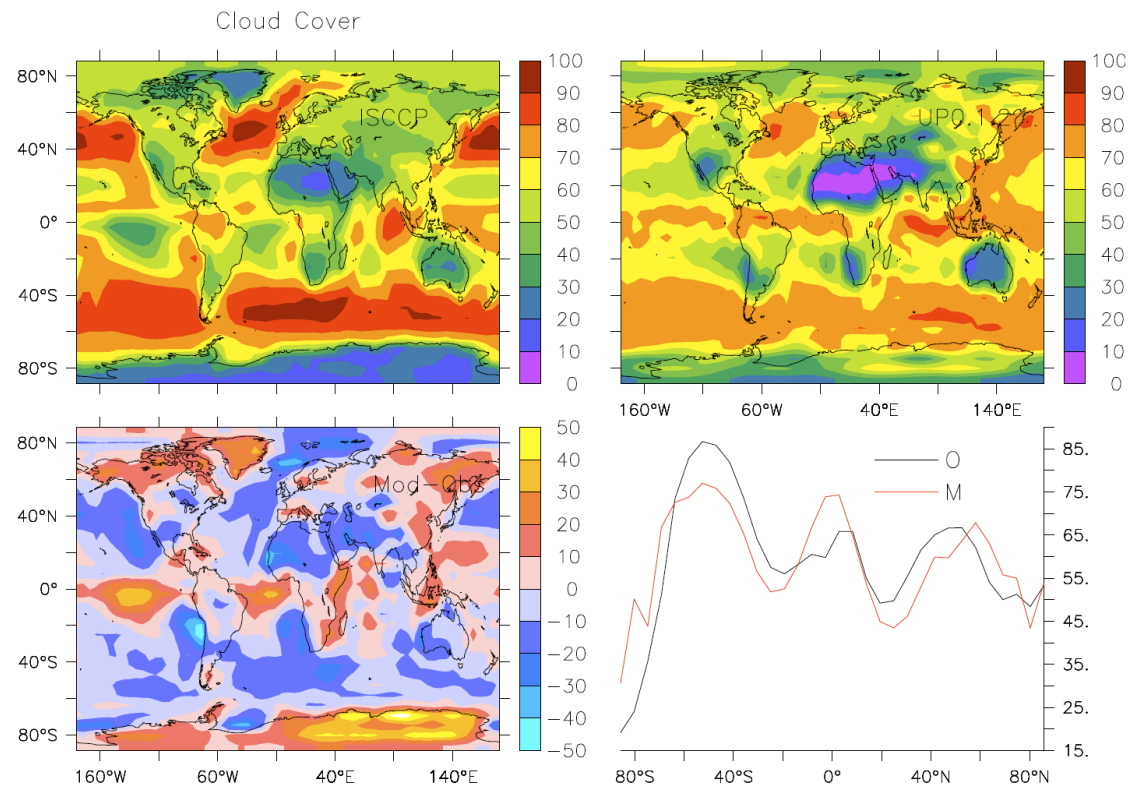


Figure 11: T21 Cloud Cover.

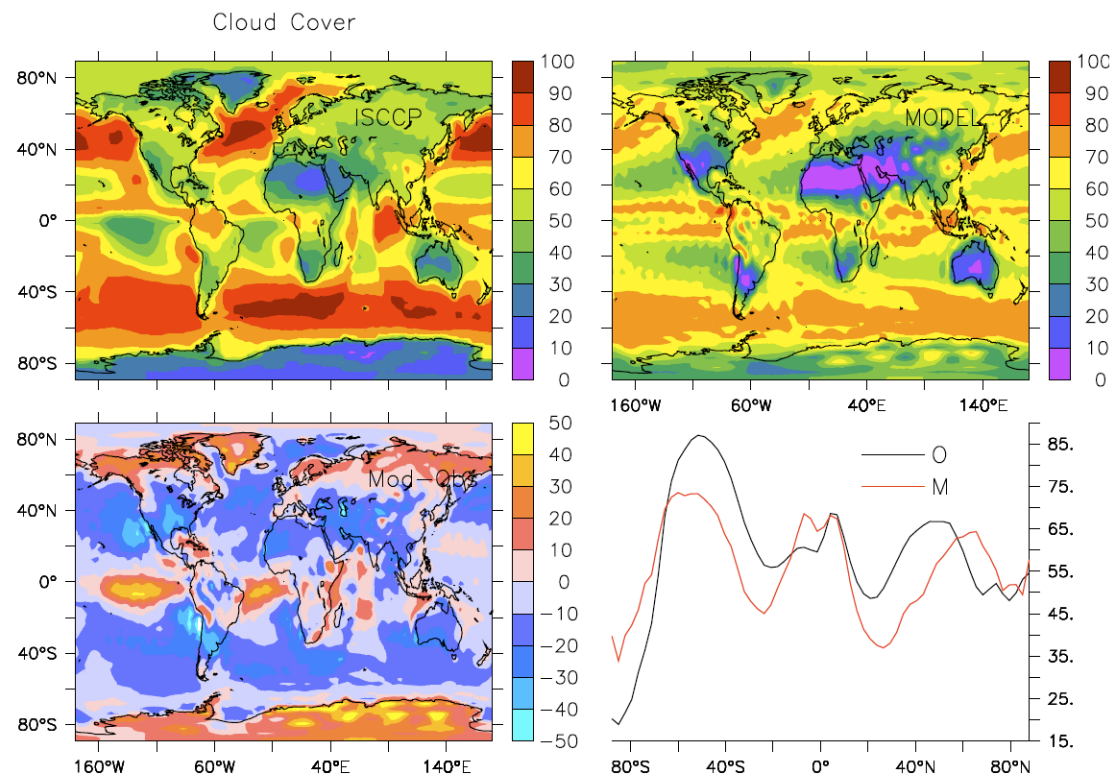


Figure 12: T42 yr 9-11

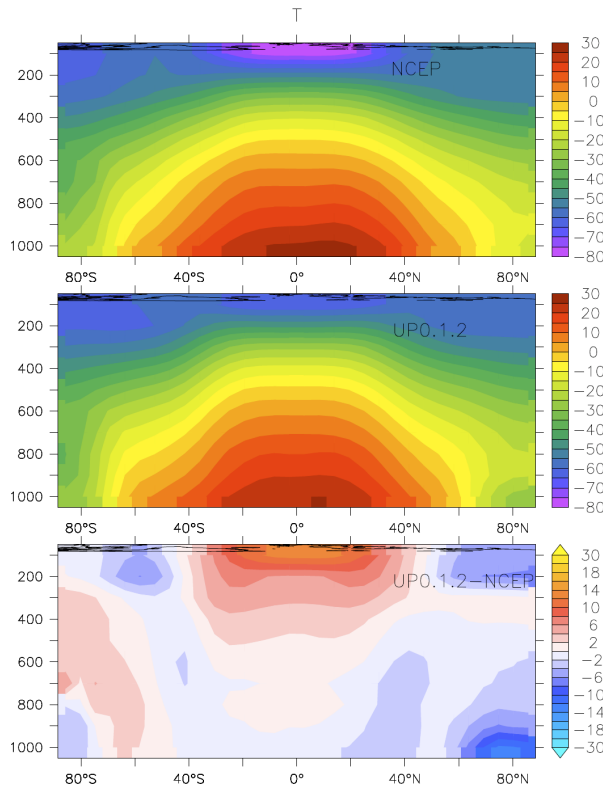


Figure 13: T21 Zonally averaged air temperature.

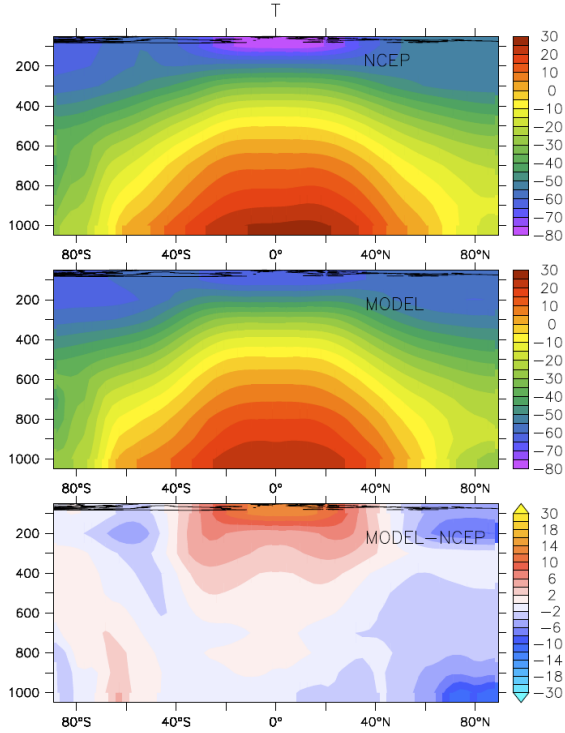


Figure 14: T42

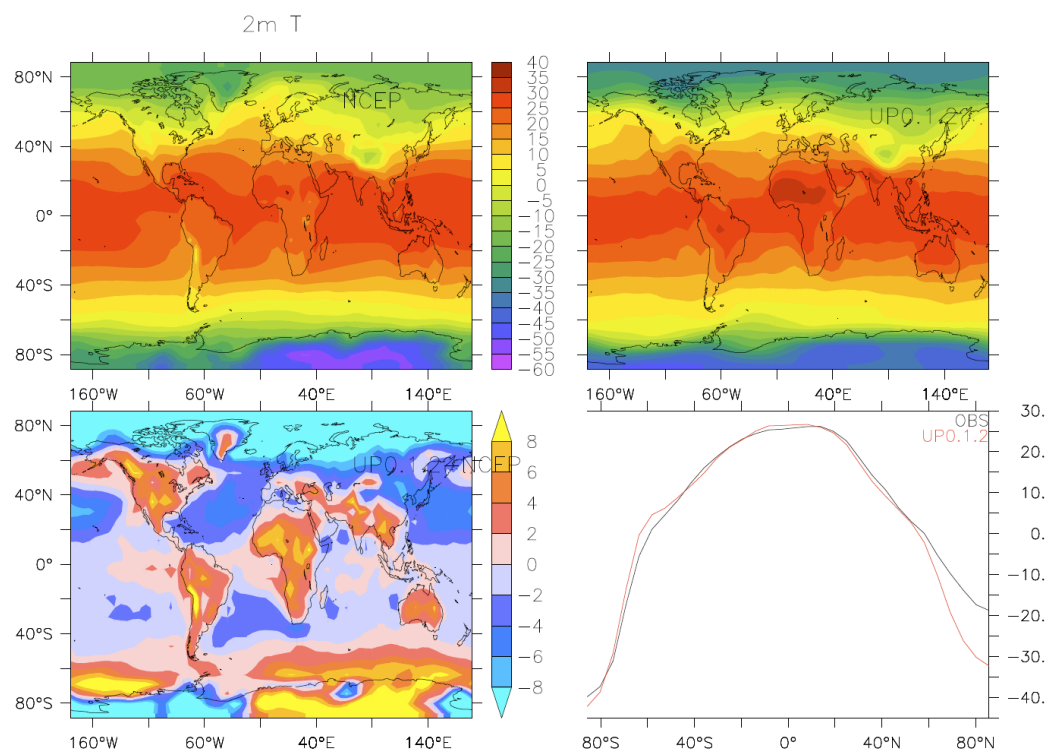


Figure 15: T21 Surface air temperature. Annual mean.

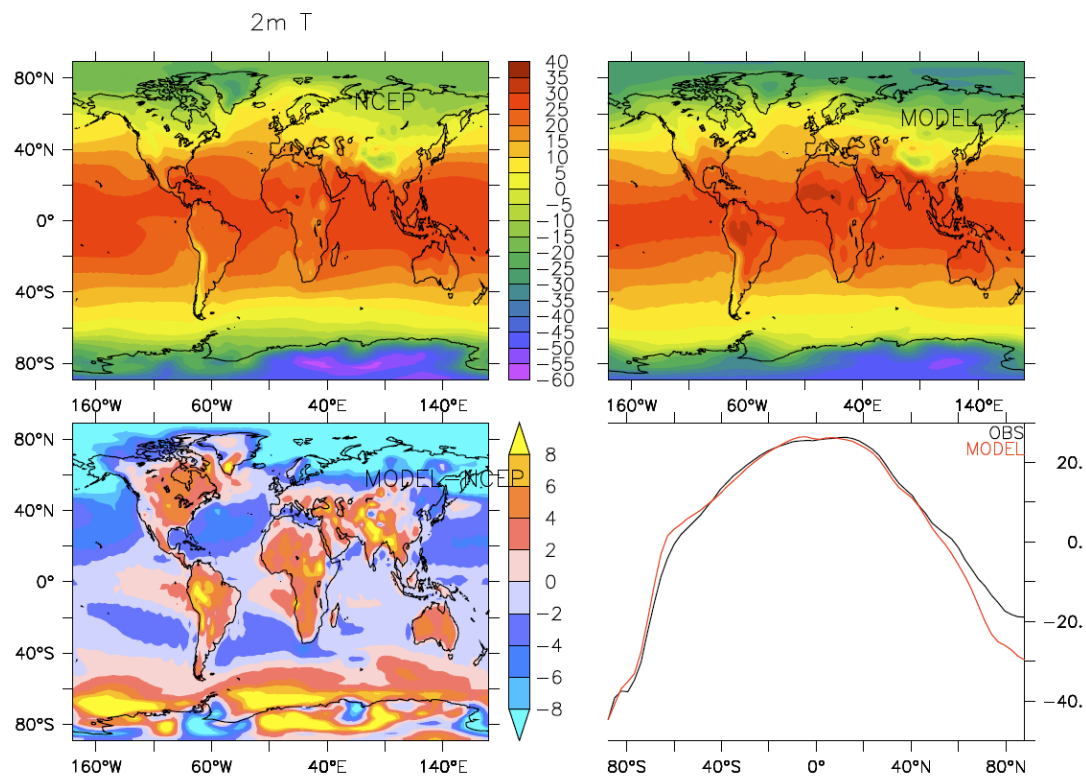


Figure 16: T42

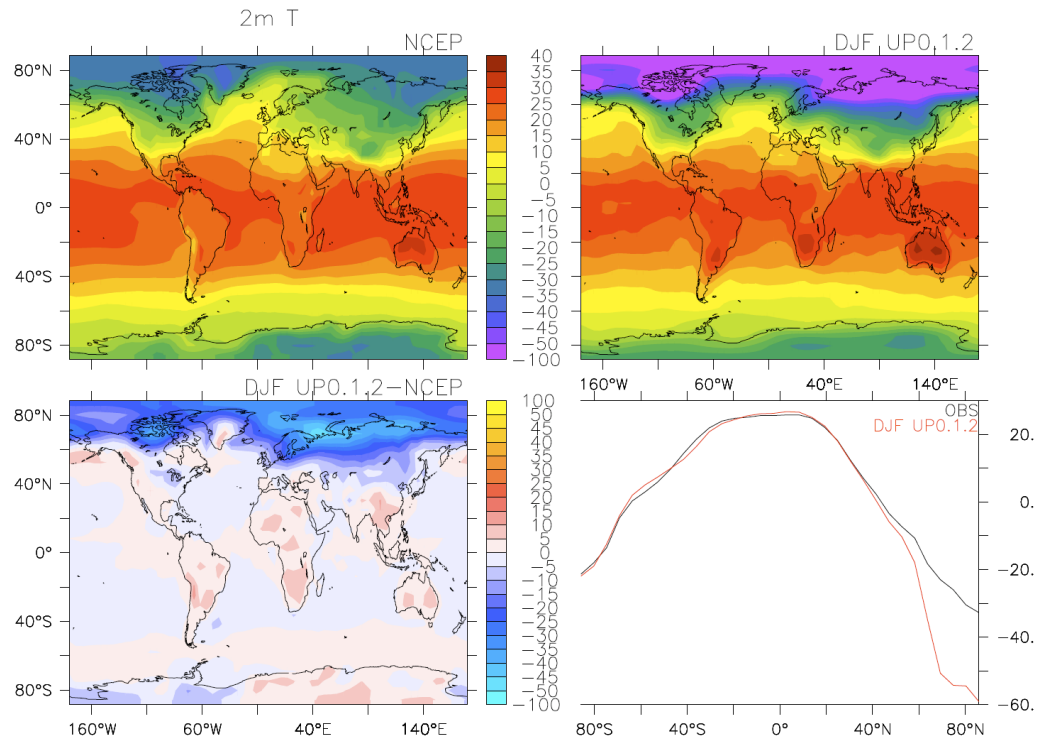


Figure 17: T21 Surface air temperature DJF

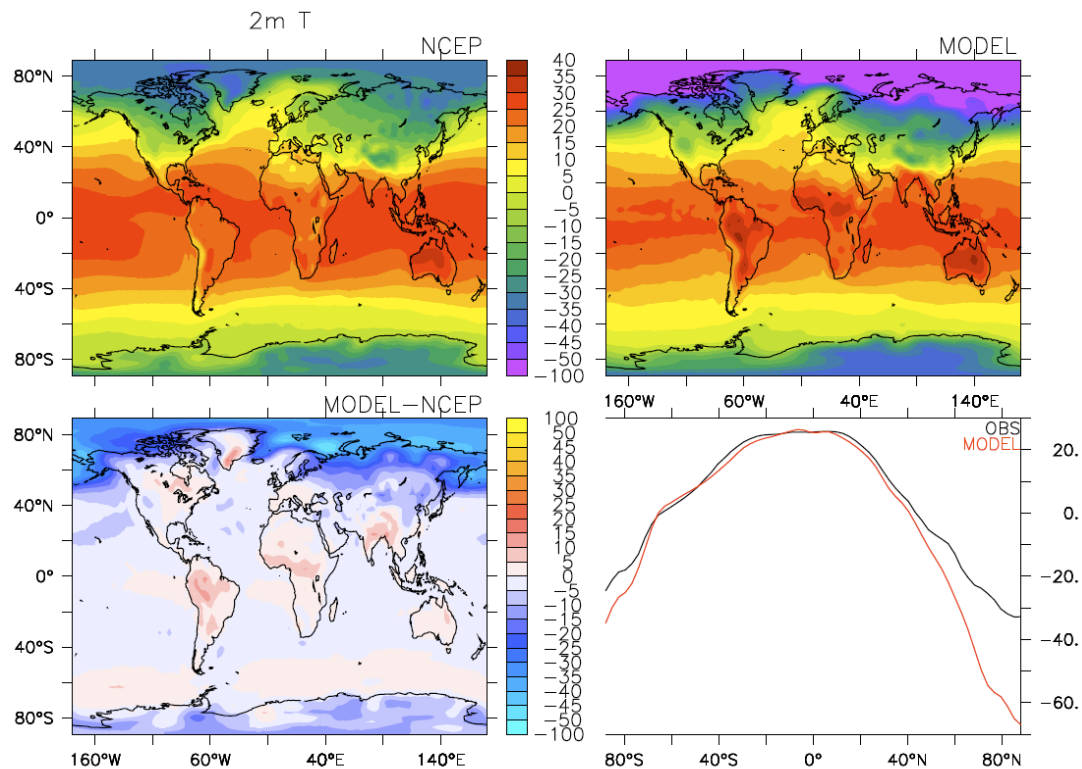


Figure 18: T42

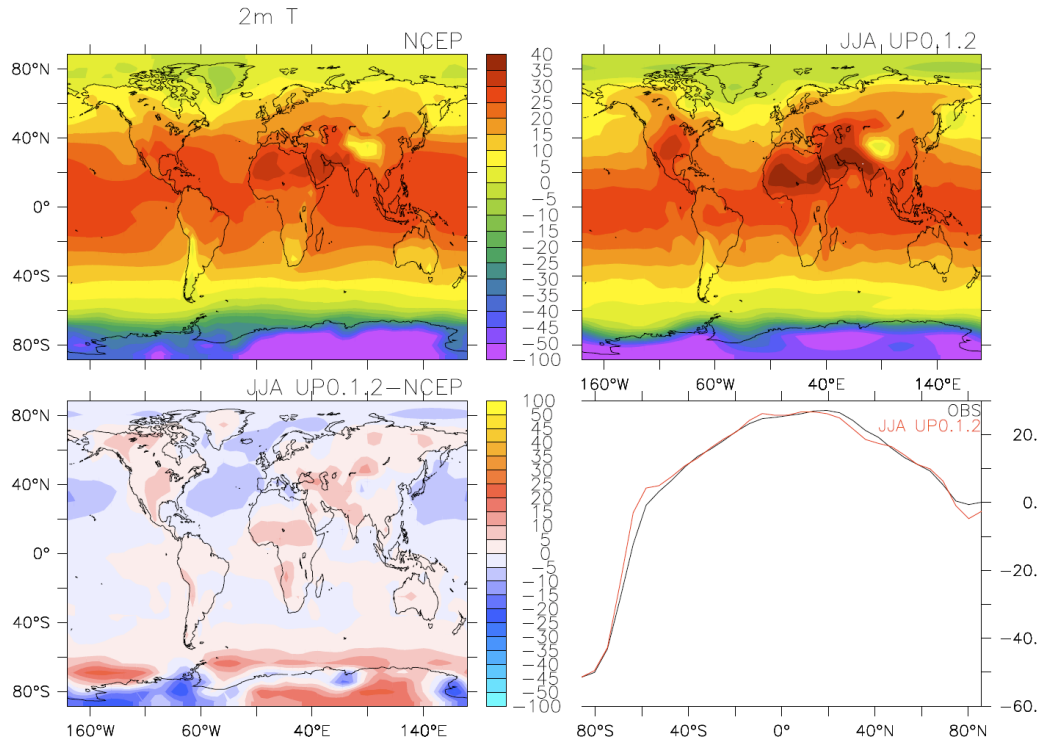


Figure 19: T21 Surface air temperature JJA

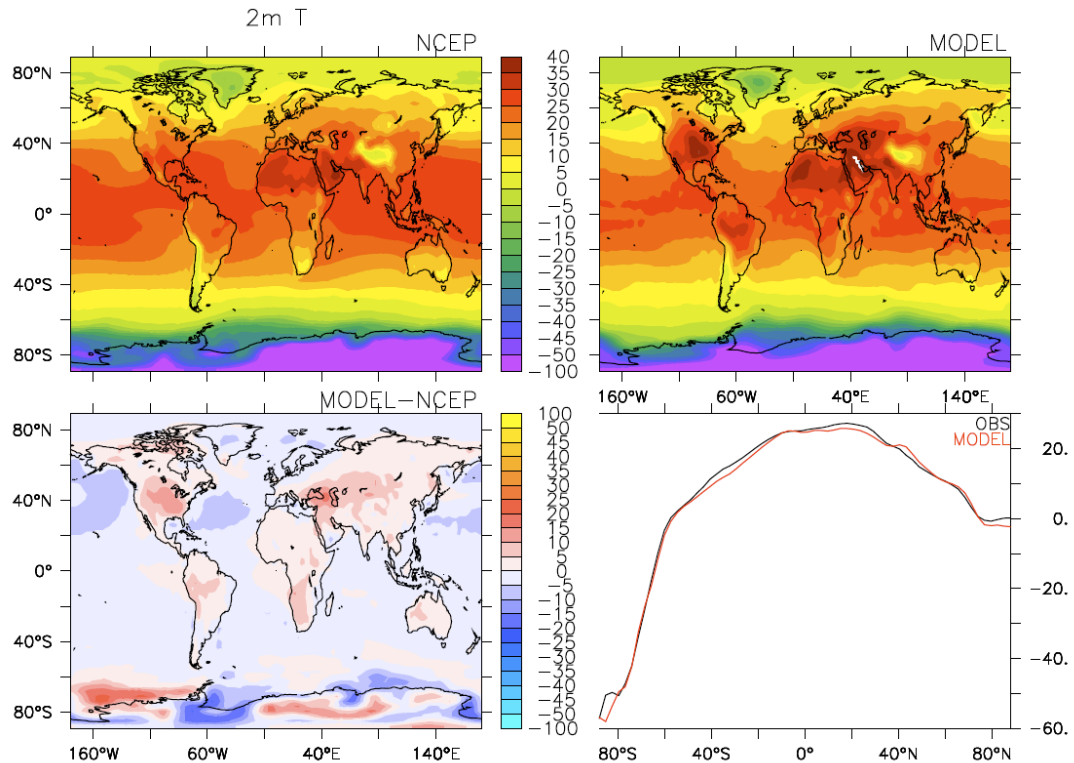


Figure 20: T42

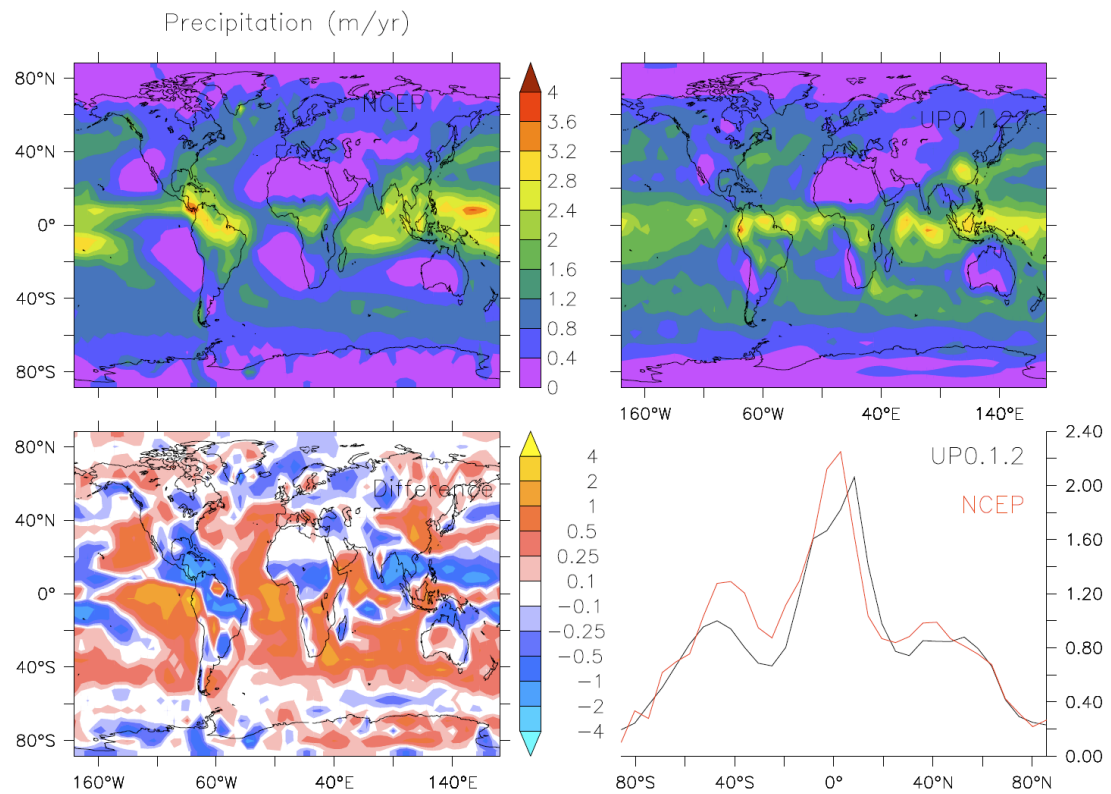


Figure 21: T21 DJF Precipitation

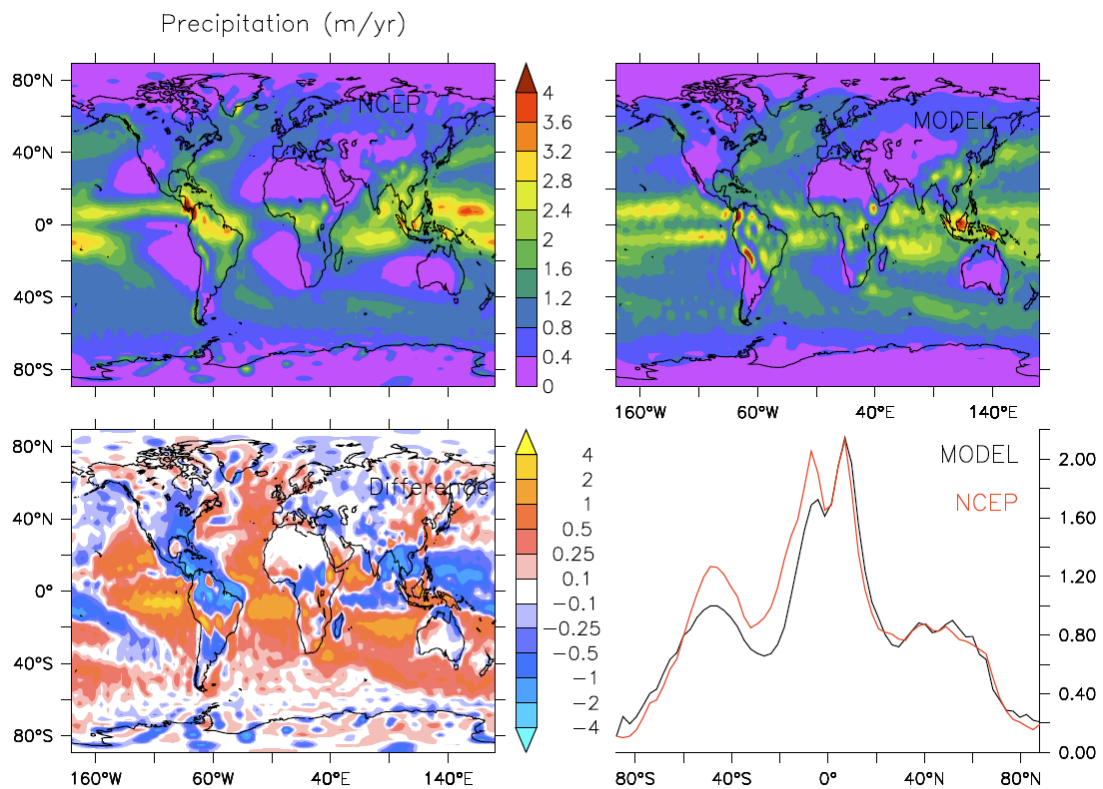


Figure 22: T42 Precipitation

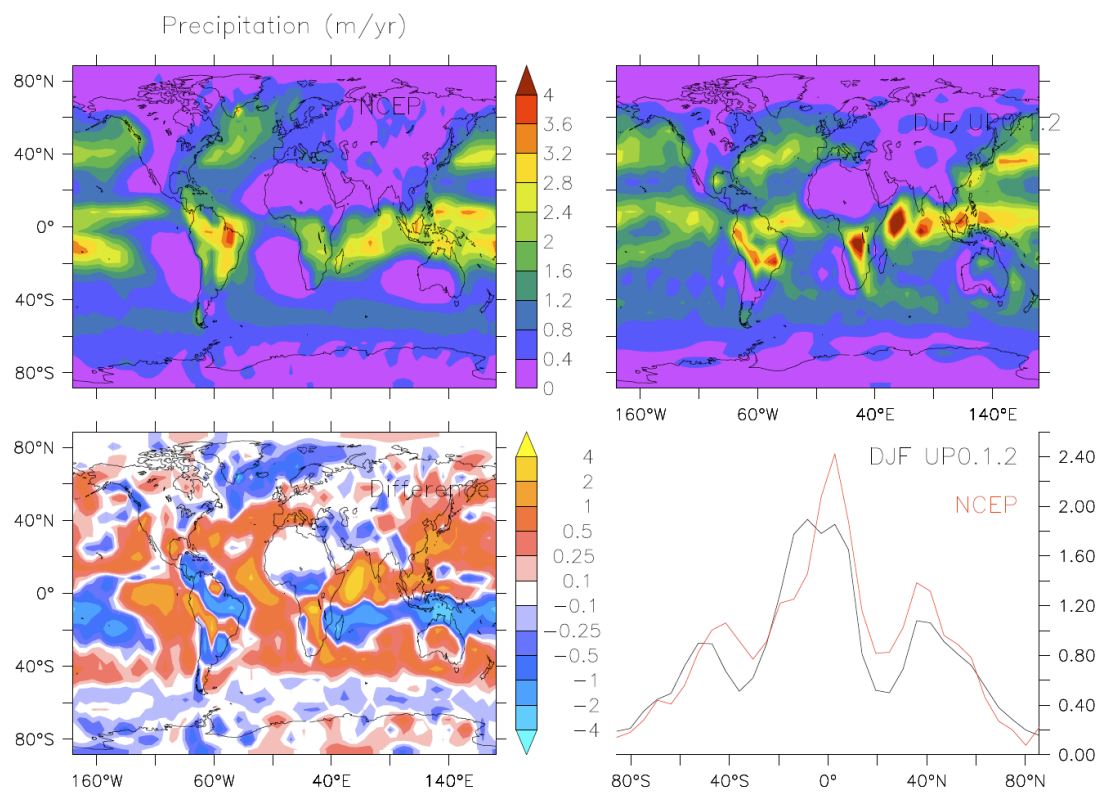


Figure 23: T21 DJF Precip.

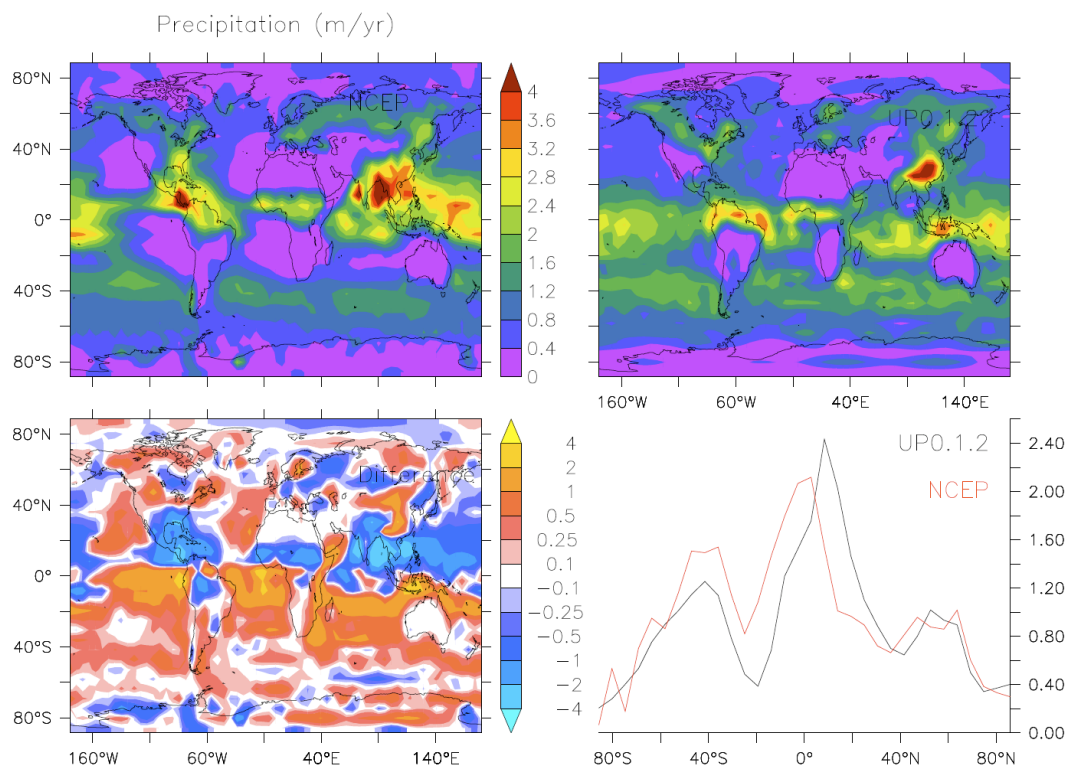


Figure 24: T21 JJA Precipitation.

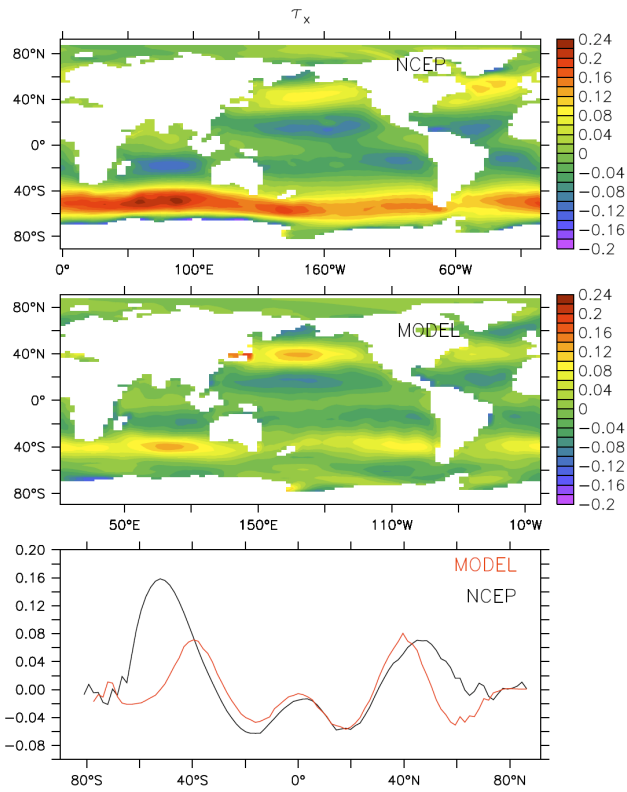


Figure 25: T21 Zonal windstress.

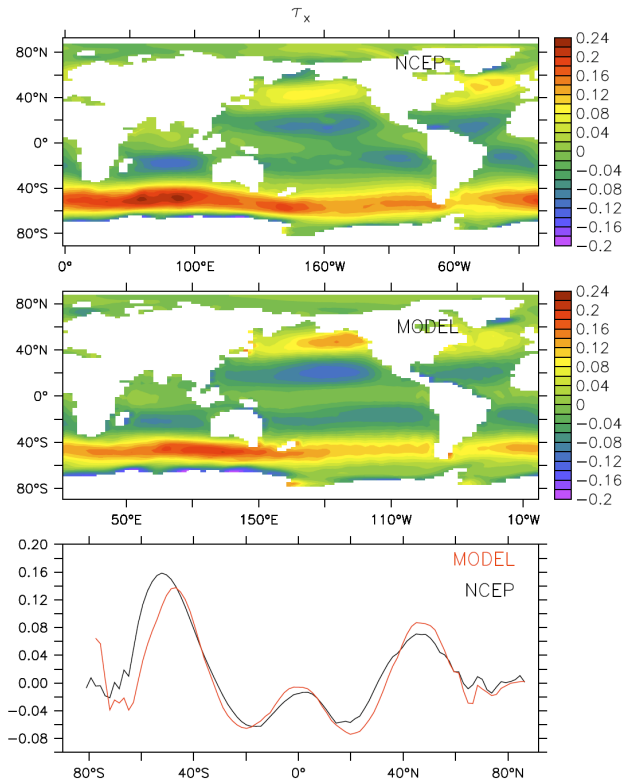
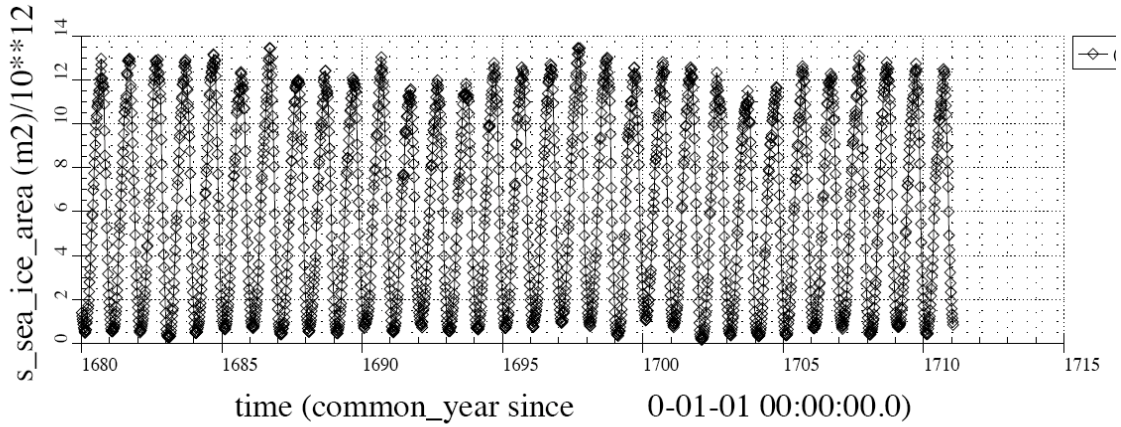
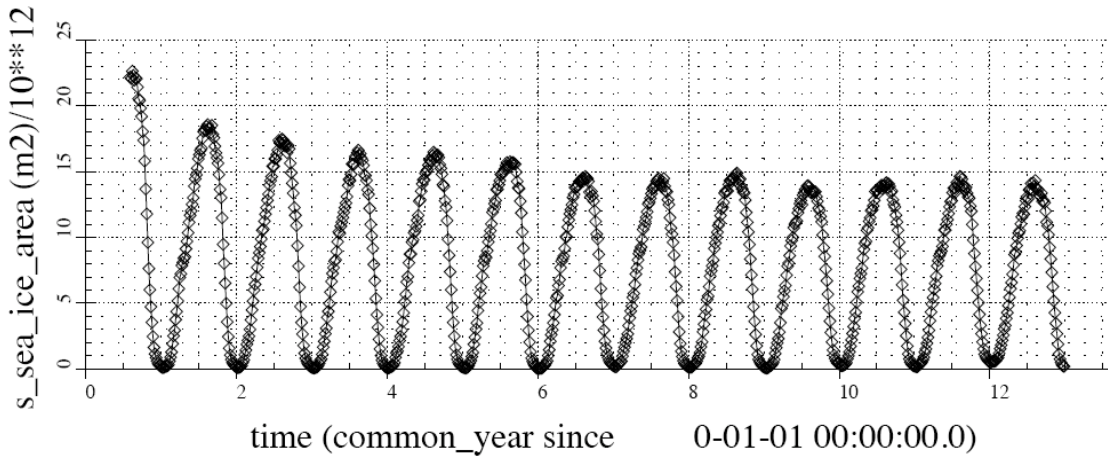


Figure 26: T42



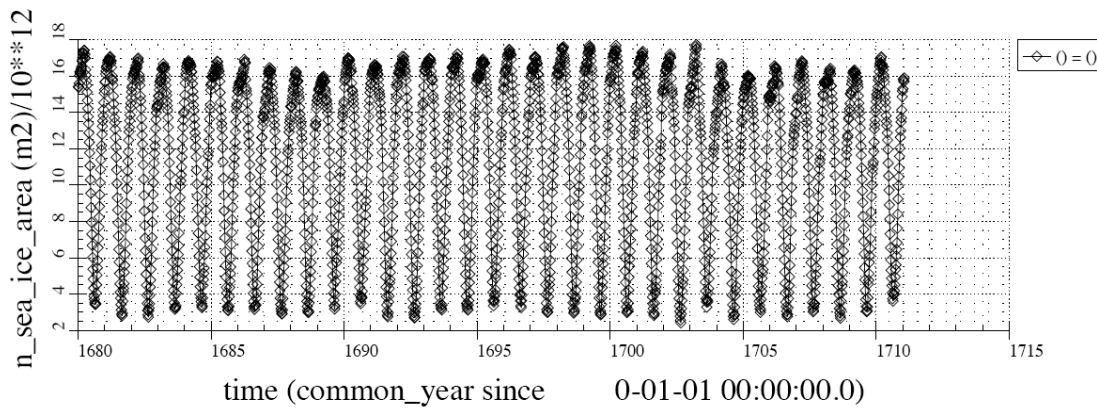
SH sea ice area

Figure 27: T21 SH sea ice area. Observations are 2(summer)-14(winter).



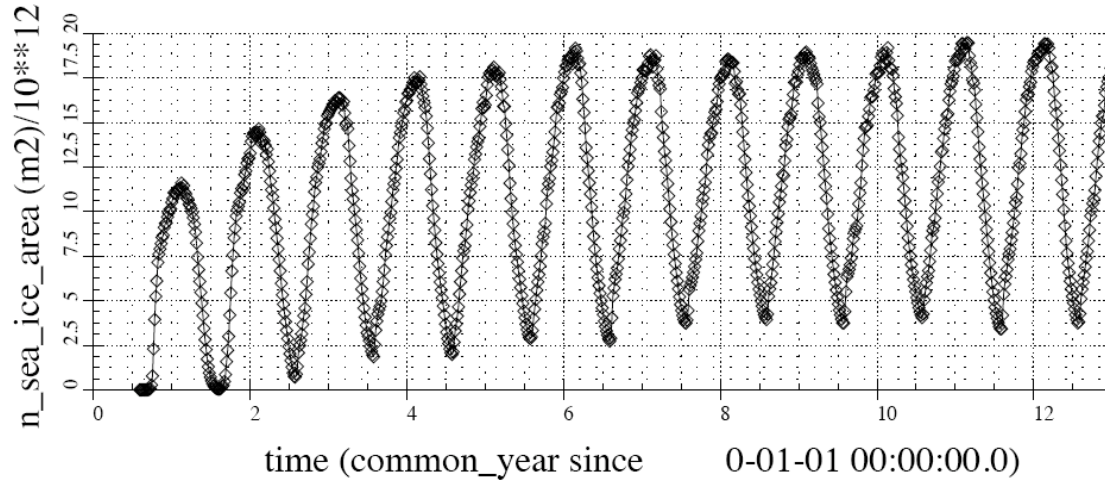
SH sea ice area

Figure 28: T42



NH sea ice area

Figure 29: T21



NH sea ice area

Figure 30: T42

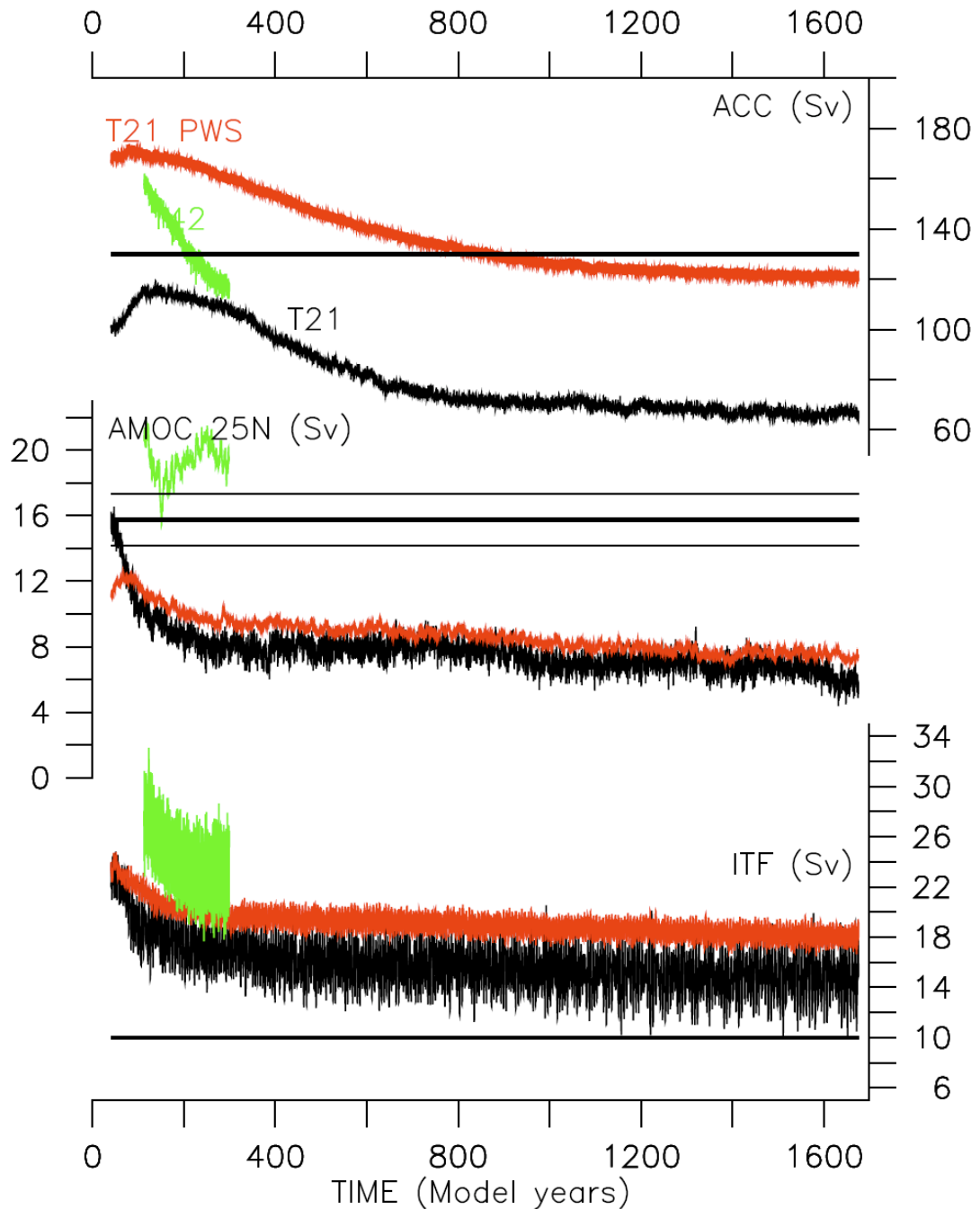


Figure 31: Ocean circulation indices. Top: Antarctic Circumpolar Current (ACC). Center: Annual mean Atlantic Meridional Overturning Circulation (AMOC) at 25N. Indonesian Throuflow (ITF). T21 (black), T42 (green) and T21 with prescribed NCEP wind stress (T21 PSW, red).

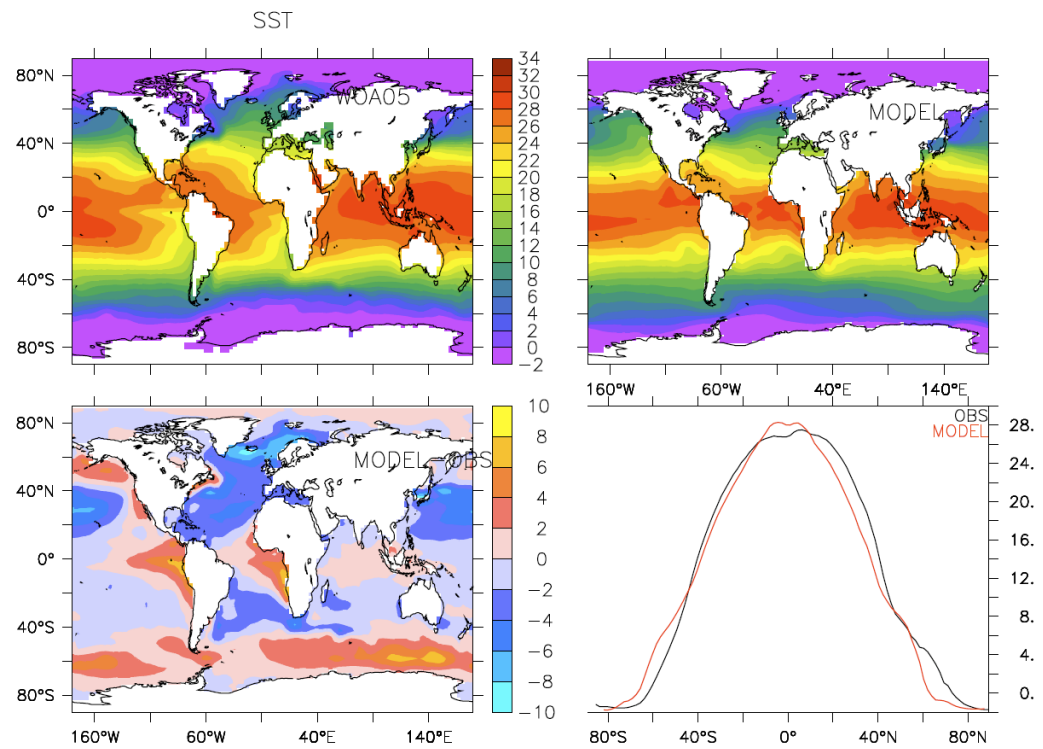


Figure 32: T21: SST

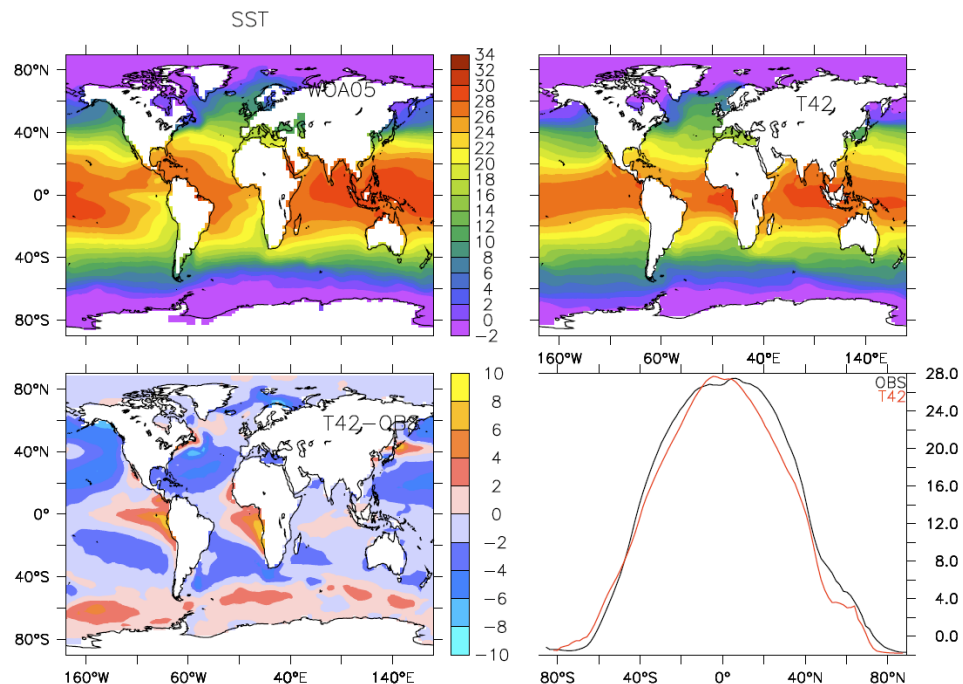


Figure 33: T42

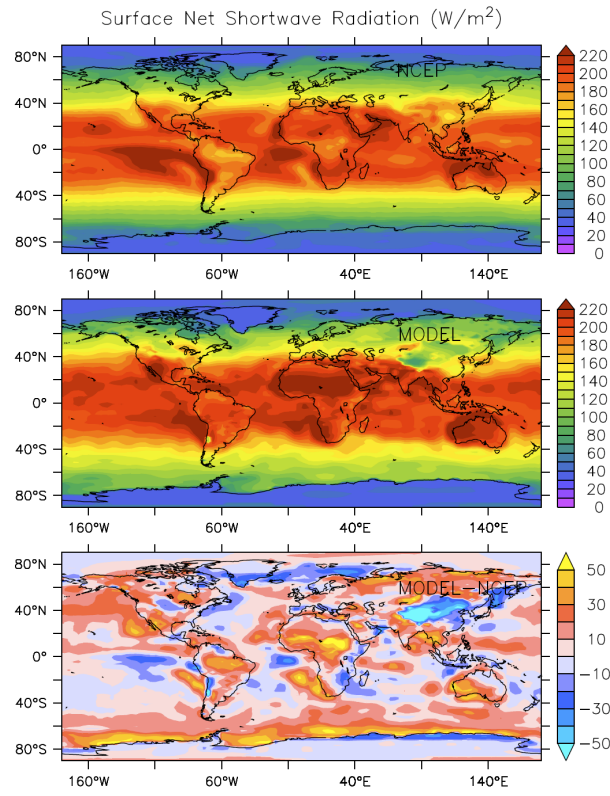


Figure 34: T21 SSW

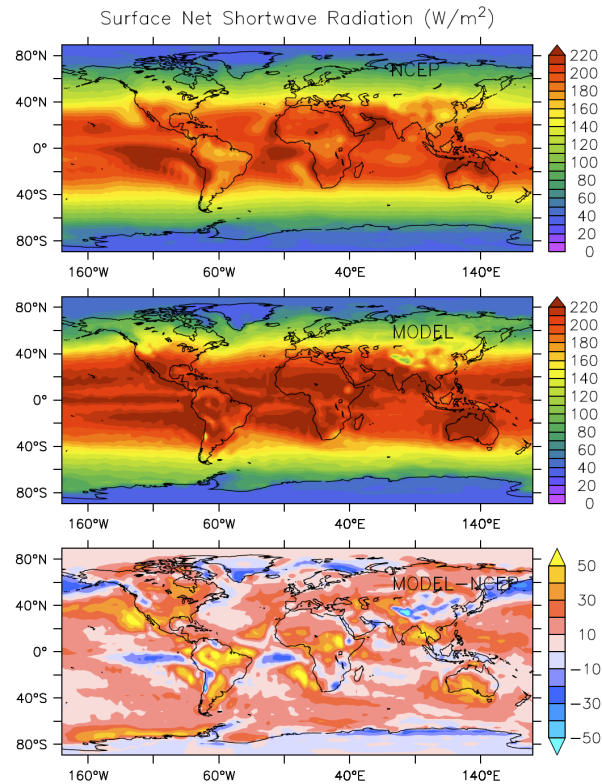


Figure 35: T42

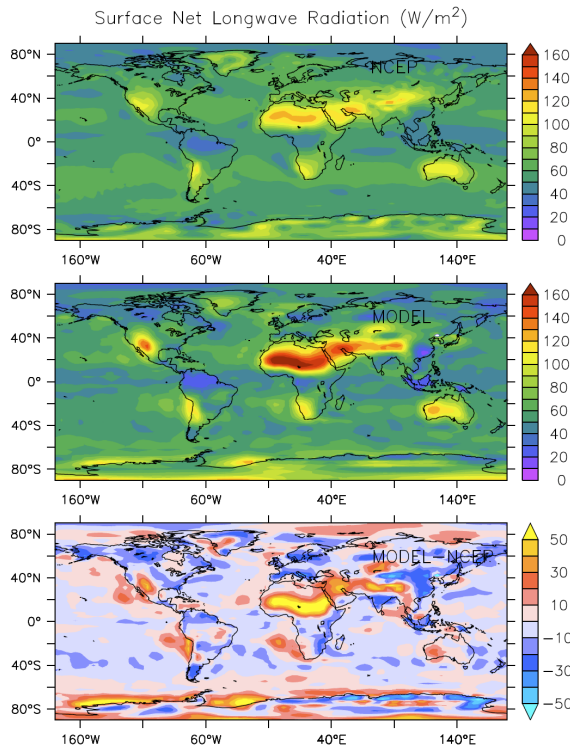


Figure 36: T21 SLW

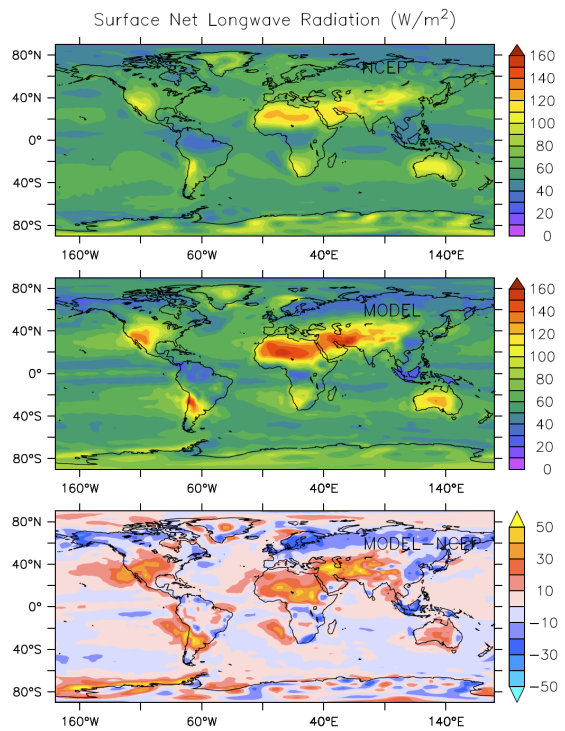


Figure 37: T42

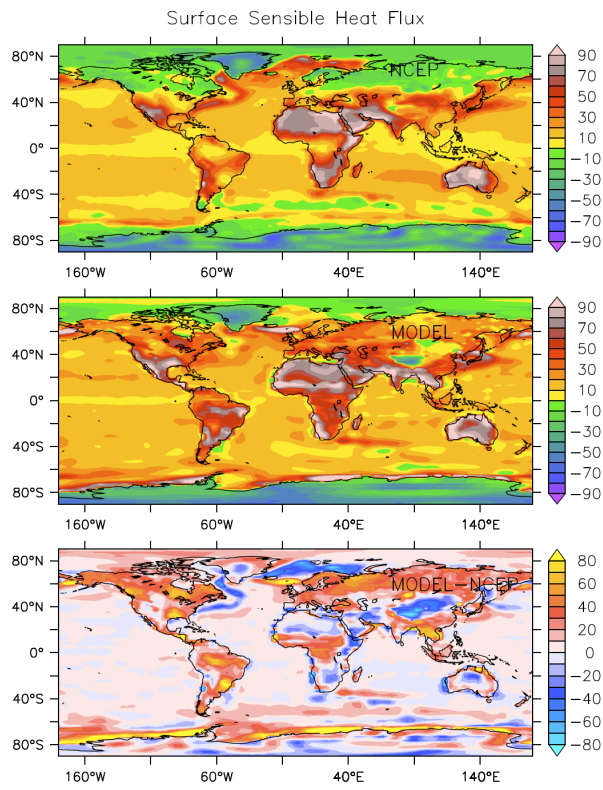


Figure 38: T21 SSH

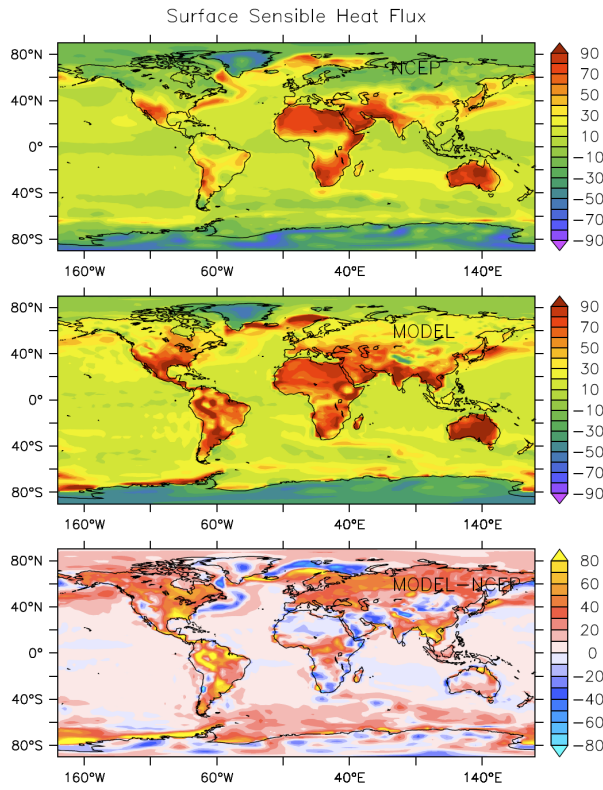


Figure 39: T42

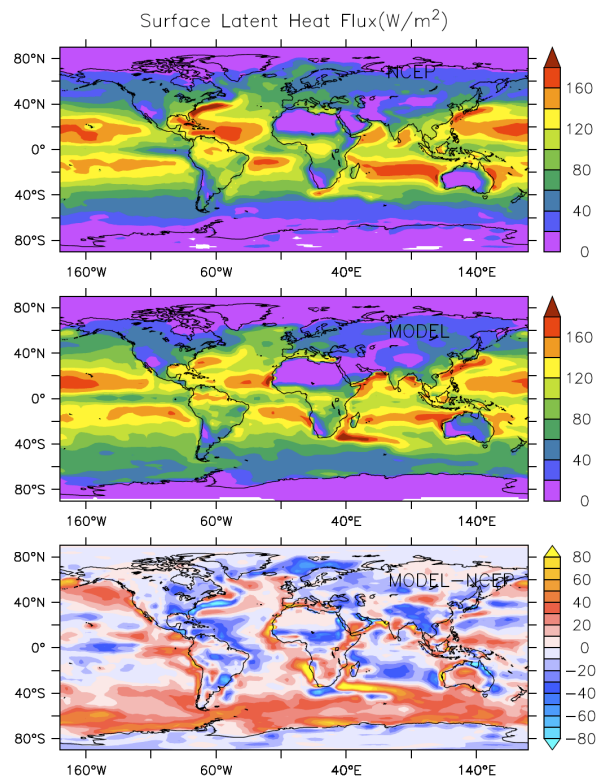


Figure 40: T21 SLH

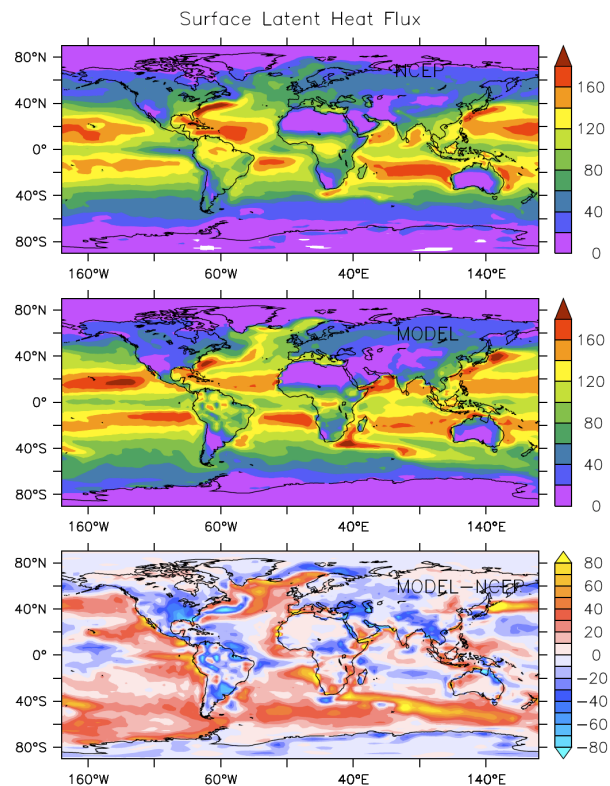


Figure 41: T42

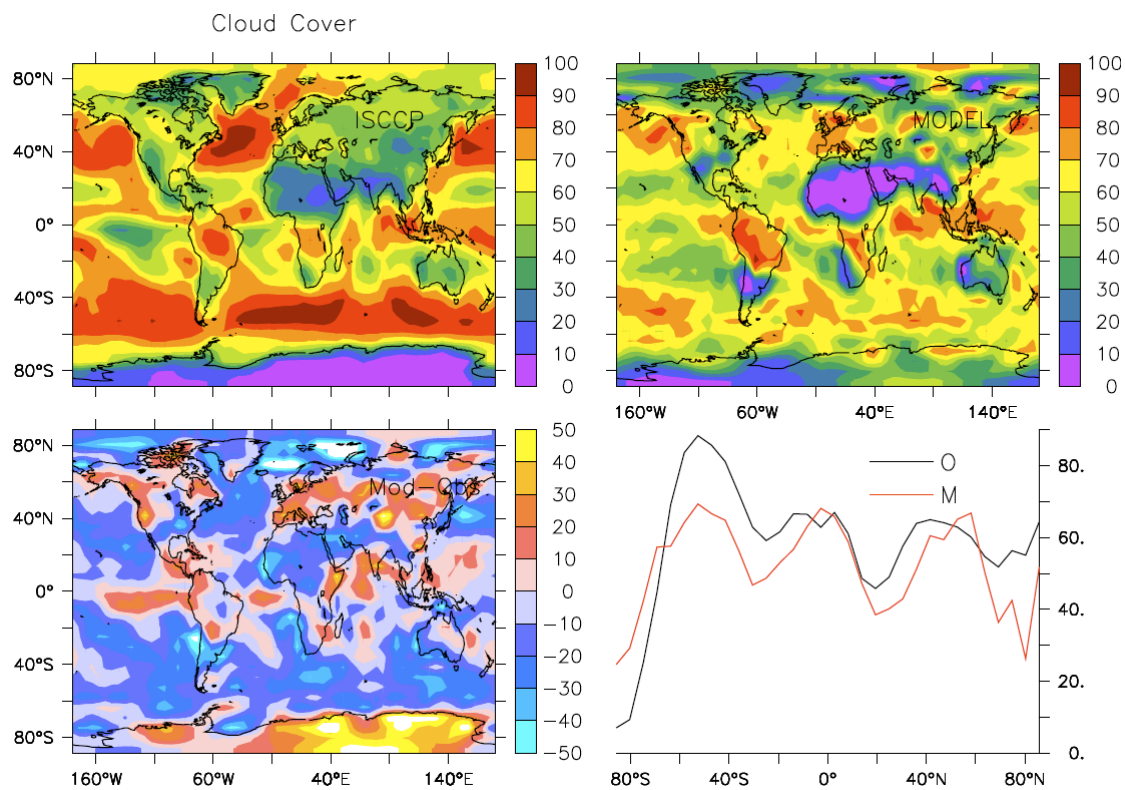


Figure 42: T21 DJF Cloud Cover

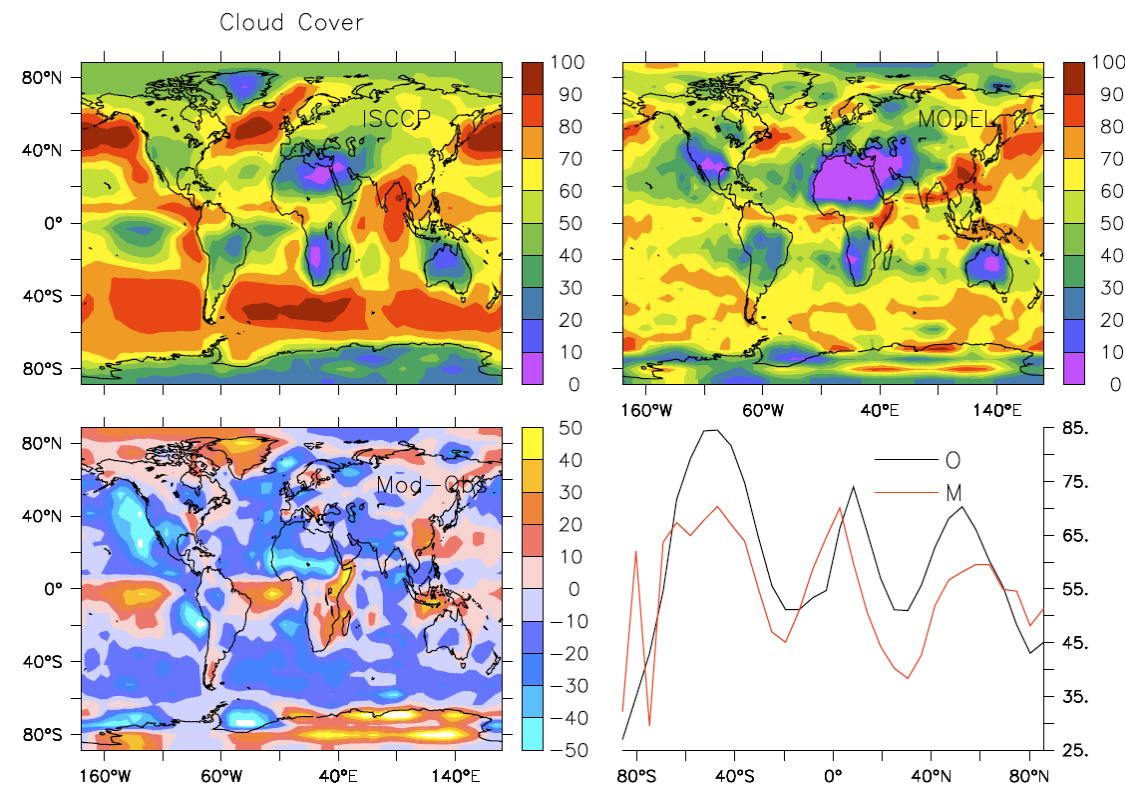


Figure 43: T21 JJA Cloud Cover

REFERENCES

- Jones, P. W. (1999), First- and second-order conservative remapping schemes for grids in spherical coordinates, *Monthly Weather Review*, 127(9), 2204-2210.
- Lunkeit, F., M. Bottinger, K. Fraedrich, E. Jansen, E. Kirk, A. Kleidon, and U. Luksch (2007), Planet Simulator Reference Manual Version 15.0.
- Weaver, A. J., M. Eby, E. C. Wiebe, C. M. Bitz, P. B. Duffy, T. L. Ewen, A. F. Fanning, M. M. Holland, A. MacFadyen, H. D. Matthews, K. J. Meissner, O. Saenko, A. Schmittner, H. X. Wang, and M. Yoshimori (2001), The UVic Earth System Climate Model: Model description, climatology, and applications to past, present and future climates, *Atmos.-Ocean*, 39(4), 361-428.